THE INFLUENCE OF TILTING PAD BEARING CHARACTERISTICS ON THE STABILITY OF HIGH SPEED ROTOR-BEARING SYSTEMS

J. C. Nicholas, Visiting Assistant Professor
E. J. Gunter, Professor
L. E. Barrett, Research Engineer

Department of Mechanical and Aerospace Engineering
School of Engineering and Applied Science
University of Virginia
Charlottesville, Virginia

ABSTRACT

This work develops a computer design optimization for tilt pad bearings. A stability analysis is carried out for an 11-stage centrifugal compressor supported by 8 geometrically different pairs of 5-pad tilt pad bearings. The compressor represents a typical class of machine with a relatively flexible shaft often encountered in industry. The zero preloaded, centrally pivoted, load on pad bearing design provides the best stability characteristics to the compressor. Increasing preload and/or offset from this design decreases stability. Pad loading makes little difference at high Sommerfeld numbers. From the results of the stability analysis, a stability parameter is deduced that provides a quick design guide to machine stability for tilt pad bearings. A critical speed and unbalance response analysis is undertaken for the compressor with the zero preload, centrally pivoted, load on pad bearings. This bearing design also provides good unbalance response characteristics to the compressor system.

NOMENCLATURE

c_b	=	$R_v - R$, tilt pad bearing assembled radial clearance in line with a pivot (L)
c_p	=	$R_p - R$, pad radial clearance (L)
C_d	=	internal friction, internal damping or hysteresis (FTL^{-1})
C_{xx}, C_{yy}	=	horizontal, vertical bearing damping (FTL^{-1})
$\bar{C}_{xx}$, $\bar{C}_{yy}$	=	$C_{xx}(\omega_j c_p/W_T)$, $C_{yy}(\omega_j c_p/W_T)$, horizontal, vertical dimensionless damping coefficients
D	=	journal diameter (L)
e	=	journal eccentricity (L)

f	=	ω_j/ω_{cr}, frequency ratio
K_s	=	fundamental shaft stiffness (FL^{-1})
K_{xx}, K_{yy}	=	horizontal, vertical bearing stiffness (FL^{-1})
$\bar{K}_{xx}$, $\bar{K}_{yy}$	=	$K_{xx}(c_p/W_T)$, $K_{yy}(c_p/W_T)$, horizontal, vertical dimensionless stiffness coefficients
$\bar{K}$	=	$\dfrac{K_{xx} + K_{yy}}{K_s}$, stiffness ratio
L	=	bearing length (L)
m'	=	journal mass (FT^2L^{-1})
m_b	=	$1 - (c_b/c_p)$, bearing preload factor
N, N_s	=	shaft rotational speed (RPM), (RPS)
$N_{1, 2, 3}$	=	first, second, third critical speed (RPM)
O_b, O_j	=	bearing, journal center
P_s	=	$2R_s \|1 - R_f\|$, stability parameter
Q	=	aerodynamic cross coupling (FL^{-1})
R, R_v	=	radius of journal, radius from bearing center to pivot (L)
R_p	=	pad radius of curvature (L)
R_f	=	K_{xx}/K_{yy}, bearing asymmetry ratio
R_s	=	K_s/K_{yy}, shaft flexibility ratio
S	=	$\dfrac{\mu N_s LD}{W_T}(R/c_p)^2$, Sommerfeld number
W_T	=	bearing external load (F)
X, Y	=	coordinate system for tilt pad bearing
α	=	θ_p/χ, bearing offset factor
ε_b	=	e/c_b, eccentricity ratio
θ_p	=	angle from leading edge of pad to pad pivot point (degrees)
μ	=	average fluid viscosity (FTL^{-2})
ξ_x, ξ_y	=	$2C_{xx}/2m'\omega_{cr}$, $2C_{yy}/2m'\omega_{cr}$, damping ratio horizontal, vertical direction
ξ_{ex}, ξ_{ey}	=	effective damping ratio, horizontal, vertical direction
$\bar{\xi}_e$	=	$1/2(\xi_{ex} + \xi_{ey})$, average effective damping ratio
χ	=	pad arc length (degrees)
ω_j, ω_{cr}	=	shaft rotational speed, rigid rotor critical speed (T^{-1})

INTRODUCTION

The tilt pad bearing has been responsible for increasing the maximum operating speed of turbo-machinery from around 6,000 RPM to 10,000 or even 14,000 RPM by virtually eliminating oil whirl instability caused by other types of fluid film bearings (1-5). As the operating speeds of rotor-bearing systems are increased, other destabilizing effects become predominate such as aerodynamic cross coupling (6-9) and internal damping (8-14). For high speed, high performance machines, proper tilt pad bearing design and/or squeeze film dampers are essential to control these instabilities (9). In many cases a properly designed tilt pad bearing with optimum bearing clearance and preload is sufficient to stabilize a multi-mass flexible rotor without the necessity of employing squeeze film dampers in the system. Although the squeeze film damper has proven to be successful in stabilizing multi-stage turborotors for high-speed operation, there has been some reluctance to use these devices. The squeeze film damper must be carefully sized for the particular rotor system in which it is to be employed. The damper may not prove to be effective if the supporting spring rate is too high or if the damper is subjected to high unidirectional or dynamic loads such as caused by compressor volute loadings or rotating unbalance forces (15).

There are many geometric variables available in tilt pad bearing design. The bearing clearance, offset factor, preload, number of pads and pad loading are all variables. This paper illustrates how the proper choice of a tilt pad bearing can greatly improve the stability of an 11-stage centrifugal compressor. The compressor design was chosen to represent a typical class of machine with a relatively flexible shaft that is often encountered in industry. Only a five pad bearing is considered as it is the most popular in industrial application. Different preloads, offsets, and pad loadings (on and between pad) will be studied.

Very little is available in the literature concerning the effects of tilt pad bearings on turbomachine stability. Warner and Soler (7) examined the stability of a single-mass flexible rotor with aerodynamic cross-coupling forces. The rotor was supported by either 4-pad tilt pad bearings or 150° fixed partial-arc bearings, both mounted in flexible damped supports. Lund (8) concluded that a 5-pad tilt pad bearing would stabilize an 8-stage centrifugal compressor that was unstably operating with plain journal bearings. Presently, the effects of tilt pad bearing preload, offset, and pad loading on the stability of turbomachinery has not been fully investigated in the literature.

STABILITY ANALYSIS

Consider the 11-stage centrifugal compressor whose cross section is shown in Figure 1. The compressor is supported by two 5-pad tilt pad bearings at the rotor ends (Figure 2). Assume the following rotor characteristics:

bearing span = 177.8 cm (70 in)
effective shaft diameter = 15.24 cm (6 in)
modulus of elasticity = 20.68×10^6 N/cm^2 (30×10^6 lb/in^2)
total rotor weight = 5782.4 N (1300 lbs)
operating speed = 10,000 RPM

With these dimensions, the fundamental shaft stiffness may be calculated based on the first critical speed (rigid supports) and mode shape.

$K_s = 4.9 \times 10^5$ N/cm (2.8×10^5 lb/in)

This compressor has been chosen to represent a typical flexible shaft design often encountered in industry.

For the tilt pad bearings, assume the following dimensions:

5 pads
$\chi = 60°$
L = 5.715 cm (2.25 in)
D = 11.43 cm (4.5 in)
N = 10,000 RPM

c_p = .1016 mm (.004 in) (pad radial clearance)
μ = 1.38×10^{-6} N-s/cm^2 (2.0×10^{-6} lb-s/in^2)
W_T = 2891 N (650 lbs)

The Sommerfeld number at the operating speed is

$$S = 1.64$$

Eight tilt pad bearing geometries will be considered. Bearing preload, offset factor, and pad loading are the variables (see Table 1). Dimensional bearing characteristics for these eight bearings are tabulated for the operating speed of N = 10,000 RPM (S = 1.64) in Table 2. These characteristics were obtained from the nondimensional tilt pad bearing curves presented by Nicholas, Gunter, and Allaire in reference (16). Sample curves for four of the eight bearings are included in the Appendix.

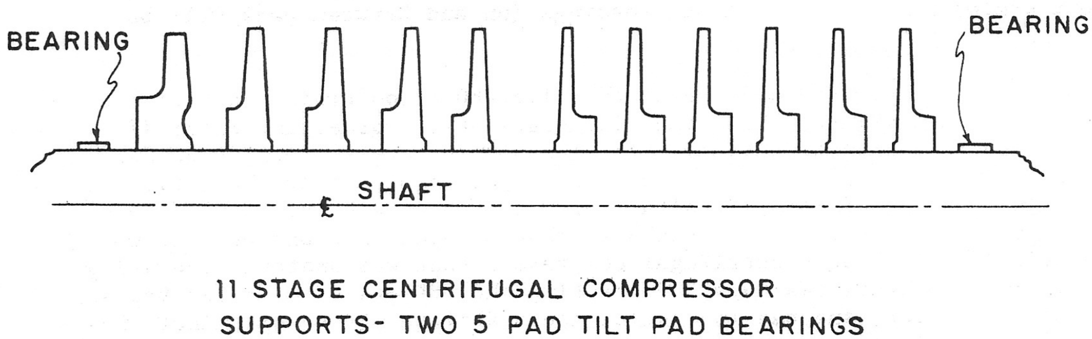

FIGURE 1 CROSS SECTION OF THE 11-STAGE CENTRIFUGAL COMPRESSOR

Bearing Number	m_b	α	Pad Loading
1	0.0	0.5	on pad
2	0.0	0.55	on pad
3	0.3	0.5	on pad
4	0.3	0.55	on pad
5	0.5	0.5	on pad
6	0.0	0.5	between pad
7	0.3	0.5	between pad
8	0.5	0.5	between pad

TABLE 1 FIVE PAD TILT PAD GEOMETRIES USED IN THE STABILITY ANALYSIS OF THE 11 STAGE COMPRESSOR

R_v = RADIUS TO PIVOT

R_p = PAD RADIUS OF CURVATURE

$R_v = R_p$ WHEN $m_b = 0.0$

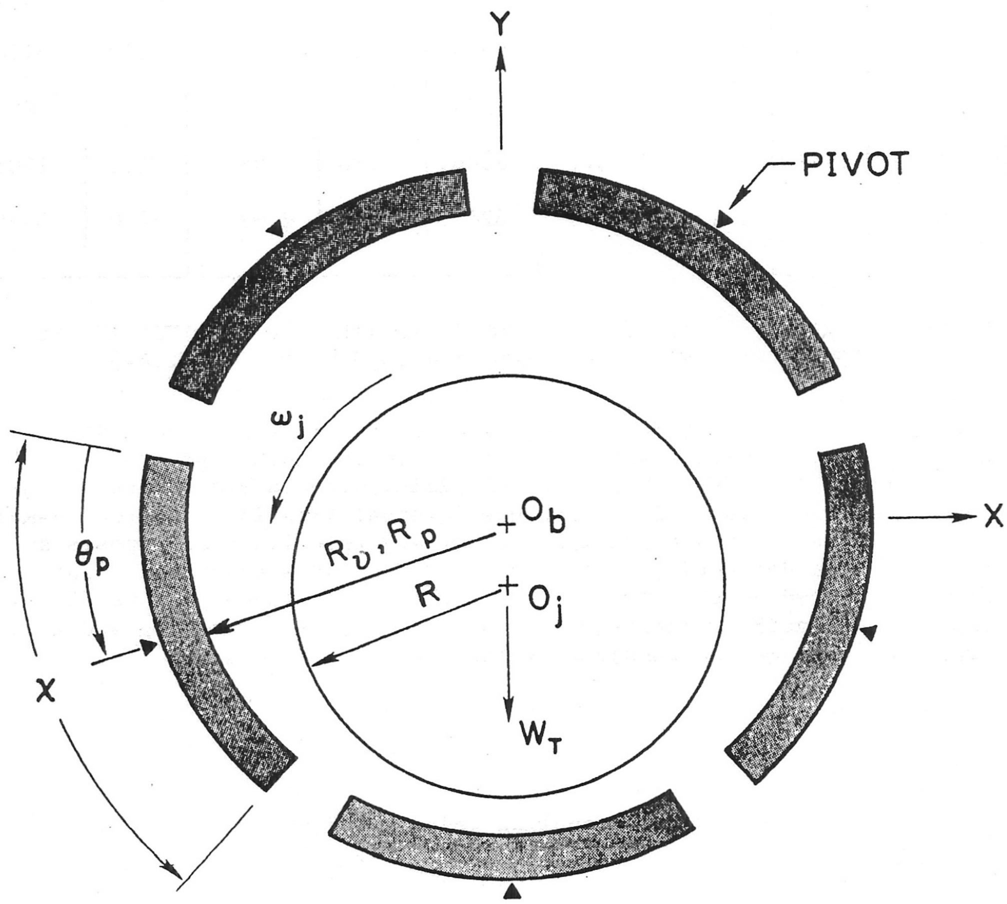

$$\alpha = \theta_p / X$$

$$m_b = 1 - c_b / c_p$$

$$c_b = R_v - R$$

$$c_p = R_p - R$$

FIGURE 2 TILT PAD BEARING SCHEMATIC

Bearing Number	(N/cm x 10^{-6})		(N-s/cm)		(lb/in x 10^{-6})		(lb-s/in)	
	K_{xx}	K_{yy}	C_{xx}	C_{yy}	K_{xx}	K_{yy}	C_{xx}	C_{yy}
1	.18	.68	1168.	1630.	.10	.39	667.	931.
2	.74	.86	1359.	1467.	.42	.49	776.	838.
3	1.51	1.79	2718.	2989.	.86	1.02	1552.	1707.
4	3.13	3.27	3804.	4077.	1.79	1.87	2172.	2328.
5	4.83	5.13	5707.	5979.	2.76	2.93	3259.	3414.
6	.28	.54	1249.	1574.	.16	.31	713.	899.
7	1.54	1.72	2986.	2986.	.88	.98	1552.	1705.
8	4.83	5.13	5972.	6243.	2.76	2.93	3410.	3565.

TABLE 2 BEARING CHARACTERISTICS FOR 5 PAD TILT PAD BEARINGS AT THE COMPRESSOR OPERATING SPEED (N = 10,000 RPM, S = 1.64)

A stability analysis was performed on the 11-stage compressor using a transfer matrix approach similar to the method presented by Lund in reference (8). All of the destabilizing effects are lumped at the rotor center. These effects include internal friction (internal damping or hysteresis) caused by shrink fits or any friction that opposes a change in the deflection of the shaft (9-12) and aerodynamic cross coupling caused in part by labyrinth seals and balance pistons (6, 9). As far as the stability analysis is concerned, internal damping and aerodynamic cross coupling may be combined by the approximate relation

$$Q = \omega_j C_d$$

where

Q = aerodynamic cross coupling (N/cm) (lb/in)
C_d = internal damping (N-s/cm) (lb-s/in)
ω_j = shaft or journal rotational speed (rad/s)

Thus, for example, say the compressor goes unstable at 10,000 RPM with C_d = 105 N-s/cm (60 lb-s/in). This is equivalent to the compressor going unstable at 10,000 RPM with $Q = 1.1 \times 10^5$ N/mm (6.28×10^4 lb/in). The stability threshold speed, N_T was determined by examining the real part of the eigenvalue. Speed dependent stiffness and damping coefficients were used for all 8 bearing geometries described in Table 1.

Figure 3 is a stability map for the 11-stage compressor. The threshold speed, N_T is plotted against internal damping, C_d. Stability threshold curves are shown for each of the 8 bearing designs. Bearing number 1 (m_b = 0.0, α = .5, on pad loading) offers the best stability characteristics. At the operating speed, the compressor can take a maximum of C_d = 142 N-s/cm (81 lb-s/in) and remain stable. This is equivalent to a maximum aerodynamic cross coupling of $Q = 1.48 \times 10^5$ N/cm (8.48×10^4 lb/in). Bearing number 6 (m_b = 0.0, α = .5, between pad loading) is a close second with bearing numbers 5 and 8 (m_b = .5) providing the worst stability. A summary of the maximum amount of C_d or Q that the compressor can tolerate and still remain stable at the operating speed is shown in Table 3. It is clear that the m_b = 0.0 bearing out performs the other preloaded cases with m_b = .33 and m_b = .5 being the second and third best respectively. Also, the α = .5 bearing is superior, as far as stability is concerned, to the α = .55 bearing. Pad loading is seen to make little difference.

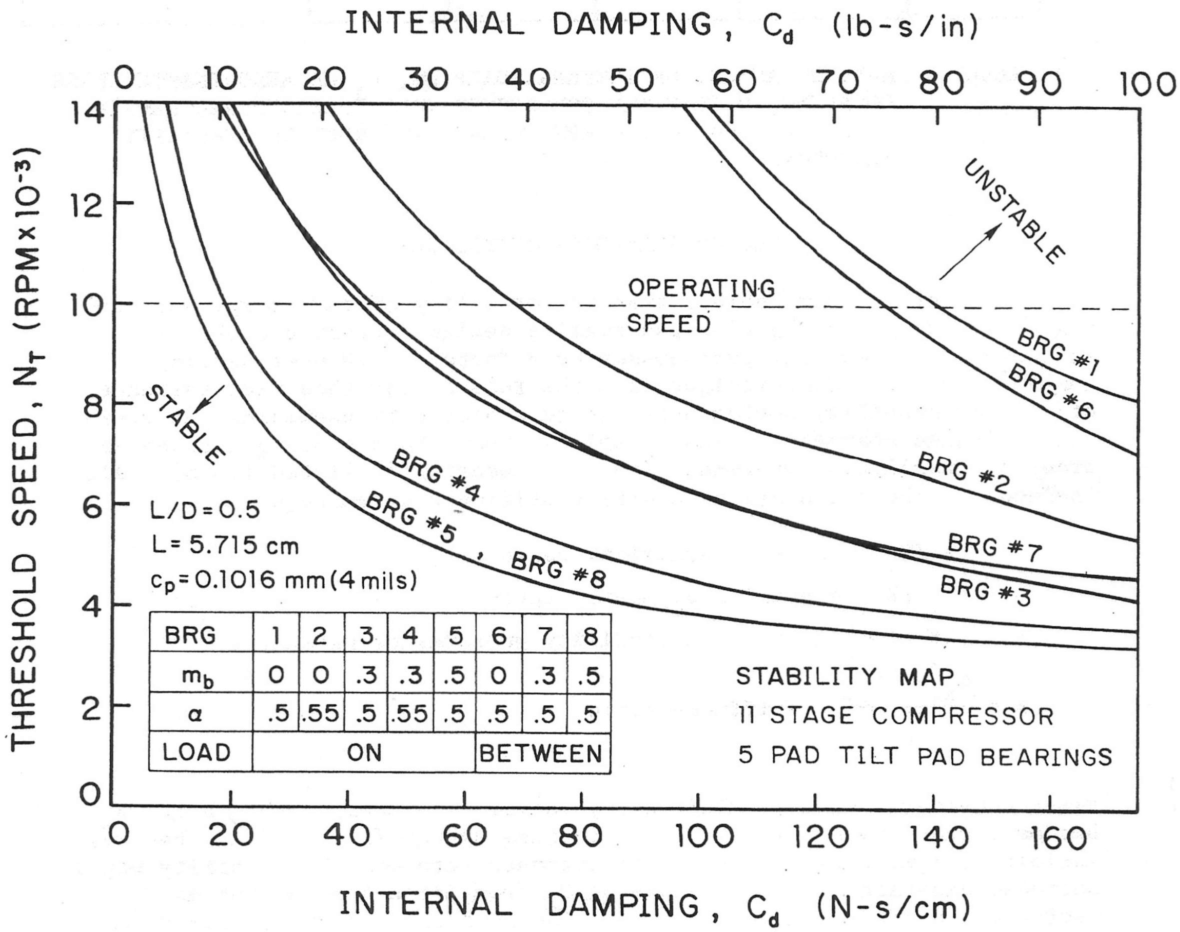

FIGURE 3 STABILITY MAP OF THE 11-STAGE CENTRIFUGAL COMPRESSOR

Bearing Number	m_b	α	Pad Loading	Q N/cm (x 10^{-3})	C_d N-s/cm	Q lb/in (x 10^{-3})	C_d lb-s/in
1	0.0	.5	ON	149.	142.	85.	81.
6	0.0	.5	BETWEEN	138.	132.	79.	75.
2	0.0	.55	ON	72.	68.	41.	39.
3	0.3	.5	ON	46.	44.	26.	25.
7	0.3	.5	BETWEEN	44.	42.	25.	24.
4	0.3	.55	ON	21.	19.	12.	11.
5	0.5	.5	ON	14.	14.	8.	8.
8	0.5	.5	BETWEEN	14.	14.	8.	8.

TABLE 3 MAXIMUM AMOUNT OF INTERNAL DAMPING, C_d OR AERODYNAMIC CROSS COUPLING, Q THAT THE COMPRESSOR WILL TOLERATE AND REMAIN STABLE AT N = 10,000 RPM (RANKED IN ORDER OF STABILITY PERFORMANCE)

BEARING STIFFNESS GUIDELINES

It is clear from Table 3 that the stability of this compressor is highly dependent on the tilt pad bearing design. Bearing number 1 increases the stability performance by a factor of 10 over bearing numbers 5 and 8. Some insight into the reasons for this wide variance of machine stability performance can be achieved by examining the bearing stiffness characteristics. Table 4 ranks the 8 bearing designs in order of stability performance (the best bearing is listed first). Also included in the table are 4 important stiffness parameters:

$$R_s = K_s/K_{yy} = \text{shaft flexibility ratio}$$
$$R_f = K_{xx}/K_{yy} = \text{bearing asymmetry ratio} \qquad (1)$$
$$P_s = 2R_s\,|1-R_f| = \text{bearing stability performance parameter}$$
$$\bar{K} = \frac{K_{xx} + K_{yy}}{K_s} = \text{stiffness ratio}$$

First consider the shaft flexibility ratio. In general, the larger R_s becomes, the more stable the rotor bearing system (12). If K_{yy} becomes infinite (rigid supports) R_s would approach zero and the stability would decrease drastically. The values of R_s from Table 4 show that as R_s increases, stability increases. Bearing numbers 1 and 6 are exceptions to this rule as they are out of order.

Another important stiffness ratio is the bearing asymmetry ratio, R_f. This is a measure of the asymmetry of the bearing. Reference (12) shows that asymmetrical bearings may inhance stability especially when $R_s > .1$. The larger R_s becomes, the more asymmetry improves stability (Figure 6, reference (12)). This trend may also be observed in Table 4. Large asymmetry is reflected in R_f values that are the farthest away from $R_f = 1.0$ (symmetric bearing). In this case, the best bearing for stability of the compressor is bearing number 1 with the lowest R_f values of .26. The stabilizing effect of stiffness asymmetry is also reported by Black in reference (13).

Bearing Number	$R_s = K_s/K_{yy}$	$R_f = K_{xx}/K_{yy}$	$P_s = 2R_s \|1-R_f\|$	$\bar{K} = \frac{K_{xx} + K_{yy}}{K_s}$
1	.72	.26	1.066	1.75
6	.90	.52	.864	1.68
2	.57	.86	.160	3.25
3	.27	.84	.086	6.71
7	.29	.90	.058	6.64
4	.15	.96	.012	13.07
5	.10	.94	.012	20.32
8	.10	.94	.012	20.32

TABLE 4 SHAFT FLEXIBILITY RATIO, R_s, BEARING ASYMMETRY RATIO, R_f, BEARING STABILITY PERFORMANCE PARAMETER, P_s AND STIFFNESS RATIO, $\bar{K}$ FOR THE 8 TILT PAD BEARING DESIGNS (RANKED IN ORDER OF STABILITY PERFORMANCE)

A combination of the shaft flexibility and bearing asymmetry ratio should produce some type of stability performance parameter. If asymmetry is present, the authors propose the parameter

$$P_s = 2R_s \, |1-R_f| \qquad (2)$$

This parameter combines the effects of asymmetry and shaft flexibility ratio. As R_s increases, P_s increases. As R_f deviates from 1.0, P_s increases. As shown in Table 4, P_s predicts the ranking of the bearings used in the compressor stability analysis. An approximate guidline for stability may be deduced from these values and Figure 3:

$$\begin{array}{lll} P_s \geq .8 & \text{rotor-bearing stability} & \text{good} \\ P_s \leq .1 & \text{rotor-bearing stability} & \text{poor} \\ .1 \leq P_s \leq .8 & \text{rotor-bearing stability} & \text{marginal} \end{array} \qquad (3)$$

The advantage of this stability performance parameter is that it is relatively simple to calculate while combining the effects of asymmetry and shaft flexibility ratio. This parameter is not meant to be rigidly adhered to. However, it may be used as a relative design parameter when a full stability analysis is impractical.

The final parameter listed in equation (1) is $\bar{K}$, the stiffness ratio. This parameter is used by Black (13) and is equal to twice the bearing stiffness divided by the shaft stiffness. This is assuming that both bearings of a two bearing rotor are the same. If not, the average may be used. For the case of asymmetry in the X-Y directions, again an average value is used as in equation (1). This parameter may also be employed as a stability guideline. Obviously, as $\bar{K}$ increases, stability decreases (Table 4). Rotor-bearing systems with stiffness ratios of around 1.0 or 2.0 should exhibit good stability characteristics. On the other hand, systems with $\bar{K}$ values greater than 6.0 should exhibit poor stability characteristics. In summary, it is clear that the bearing must be "tuned" to the shaft stiffness for favorable stability: the more flexible the shaft, the more flexible the bearings.

In examining the bearing characteristics plotted in reference (16) and the Appendix, the effects of preload, offset and pad loading become clear. Tilt pad bearings are usually used in high performance, high-speed turbomachinery where the steady-state loading is relatively light (5, 11, 17). This implies that the normal operation range of a tilt pad bearing is usually around S = 1.0 or higher. Reference (16) shows that at these high Sommerfeld numbers, on pad and between pad loading becomes irrelevant as far as changing the bearing characteristics at high Sommerfeld numbers. This may also be observed in Table 3. Bearing numbers 1, 3, and 5 are identical to bearing numbers 6, 7, and 8 except for pad loading (on pad and between pad respectively). The stability performance of bearing numbers 5 and 8 are identical, while bearing numbers 3 and 7 are almost identical and numbers 1 and 6 very close. Thus, it may be concluded that pad loading is not an important tilt pad bearing geometric variable as far as stability is concerned when operating at Sommerfeld values of $S > 1.0$.

The effect of increasing the bearing preload from $m_b = 0.0$ at high Sommerfeld numbers is to eliminate the stiffness asymmetry and to increase the bearing stiffness (Figures 10-12). The same trend is observed when the offset factor is increased from $\alpha = .5$ to $\alpha = .55$ only not quite as drastically (16). Table 3 shows that the $m_b = .33$, $\alpha = .5$ bearing is superior since it retains its stiffness asymmetry and low stiffness values. Thus, for bearing operation above S = 1.0, the zero preloaded, centrally pivoted 5-pad tilt pad bearing is superior as far as stability is concerned when compared to the $m_b = .33$, $\alpha = .55$ cases for the 11-stage compressor analyzed here.

A rather surprising result is that the centrally pivoted bearing is superior in stability compared to the $\alpha = .55$ bearing. Although the off-center pivoted bearing is more efficient as far as load capacity is concerned, its efficiency raises the bearing stiffness, thus adversely affecting the stability of the compressor.

EFFECTIVE DAMPING

Effective damping is the amount of damping supplied to the rotor system by the bearing damping and the shaft stiffness. Assuming that the multimass compressor can be represented by an equivalent modal model, the effective damping ratio is given by (18)

$$\xi_{ey} = \frac{\xi_y}{(1 + 2/R_s)^2 + (2f\xi_y)^2} \tag{4}$$

for the Y-direction. Equivalently, for the X-direction

$$\xi_{ex} = \frac{\xi_x}{(1 + 2R_f/R_s)^2 + (2f\xi_x)^2} \tag{5}$$

where

ξ_x, ξ_y = damping ratio, horizontal, vertical direction
ξ_{ex}, ξ_{ey} = effective damping ratio, horizontal, vertical direction
f = frequency ratio

Note that as R_s increases, ξ_e increases, providing good stability characteristics to the rotor-bearing system.

The effective damping ratio has been tabulated in Table 5 in both the X and Y-directions for all 8 geometrically different tilt pad bearing designs. An average value is also shown where

$$\bar{\xi}_e = 1/2\ (\xi_{ex} + \xi_{ey}) \qquad (6)$$

where values were calculated for $\omega_1 = \omega_{cr} = 419$ rad/s ($f = 1$), the rigid bearing critical speed for the first mode (see Figures 4 and 5). This value was used because equations (4) and (5) are more appropriate when analyzed in the vicinity of the first critical speed (18). Table 5 shows, as expected, that as the effective damping increases, stability becomes more favorable. In fact, the average effective damping, $\bar{\xi}_e$ predicts the ranking of the bearings.

Bearing Number	ξ_{ex}	ξ_{ey}	$\bar{\xi}_e$
1	.153	.050	.102
6	.090	.058	.074
2	.092	.050	.071
3	.060	.038	.049
7	.054	.042	.048
4	.037	.030	.034
5	.026	.022	.024
8	.026	.022	.024

TABLE 5 EFFECTIVE DAMPING FOR 5 PAD TILT PAD BEARINGS RANKED IN ORDER OF STABILITY PERFORMANCE

Effective damping is an interesting parameter in that it combines the effects of bearing damping and the shaft flexibility ratio R_s. More importantly, effective damping also provides insight concerning the unbalance characteristics of the rotor-bearing system: high effective damping means favorable unbalance response. In fact, the effective damping is approximately inversely proportional to the stiffness ratio, $\bar{K}$, (13). Thus, it is expected that tilt pad bearing number 1 which provides the best stability characteristics should also provide the best unbalance characteristics. This will be investigated further in the next section.

Undamped critical speed maps for both the horizontal X-direction and the vertical Y-direction are shown in Figures 4 and 5 for the 11-stage compressor. The bearing stiffness characteristics are also plotted for all eight 5-pad bearing designs. In both plots the bearing numbers appear in order of their stability rank. That is, bearing numbers 1 and 6, which provide good stability characteristics, have the lowest stiffness values at the operating speed. Their bearing curves cross the critical speed curves closer to the "rigid rotor" section of the map where shaft stiffness becomes large enough (bearing stiffness small enough) for the rotor to react as a rigid rotor. Bearing numbers 4, 5, and 8, which provide poor stability to the compressor, have the highest stiffness values and their curves are closest to the "rigid support" section of the map. This section is when the shaft stiffness becomes small enough and/or bearing stiffness large enough for the rotor to react as if it were on rigid supports. As the "rigid rotor" section is approached on the critical speed map, $\bar{K}$ becomes small (approaches 1.0) which is favorable to stability. Conversely, as the "rigid support" section is approached, $\bar{K}$ becomes large which is unfavorable to stability.

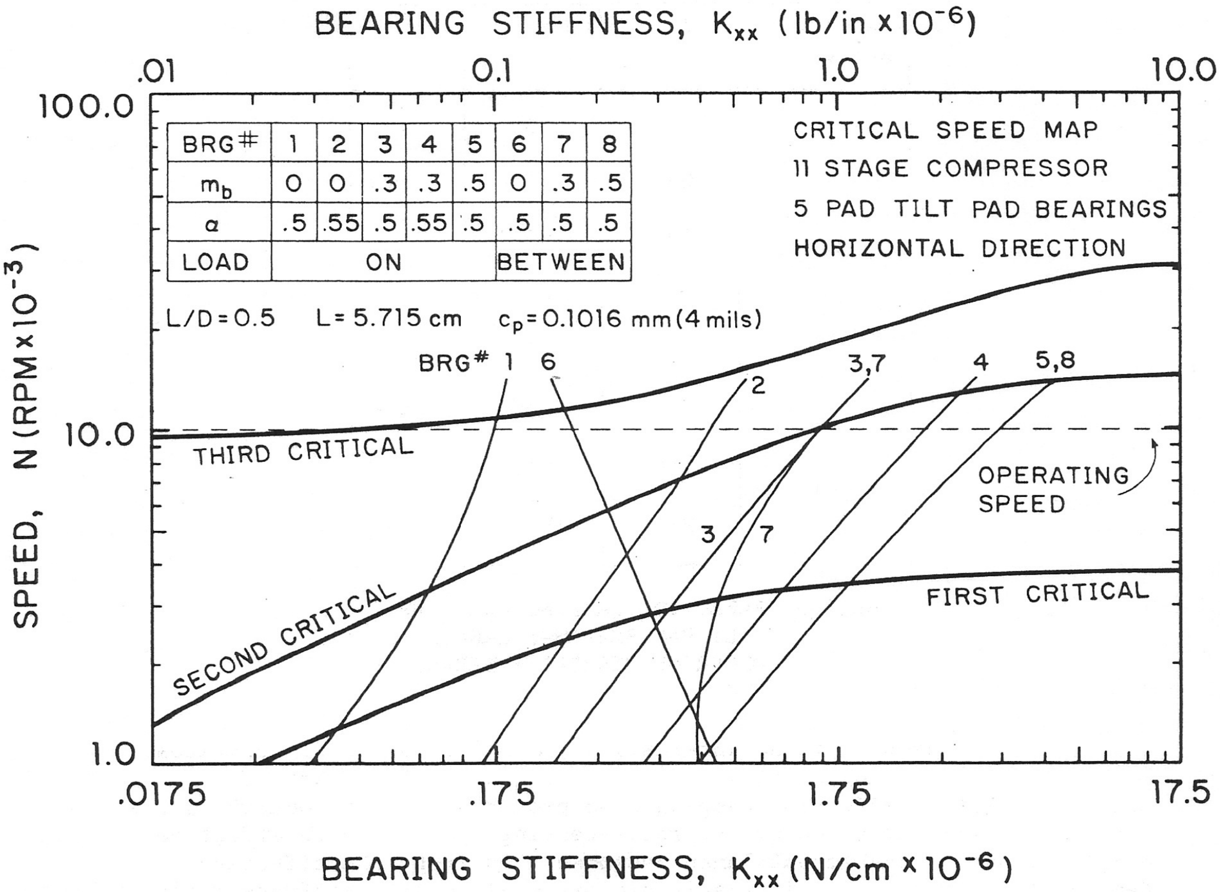

FIGURE 4 CRITICAL SPEED MAP, HORIZONTAL DIRECTION, 11-STAGE CENTRIFUGAL COMPRESSOR

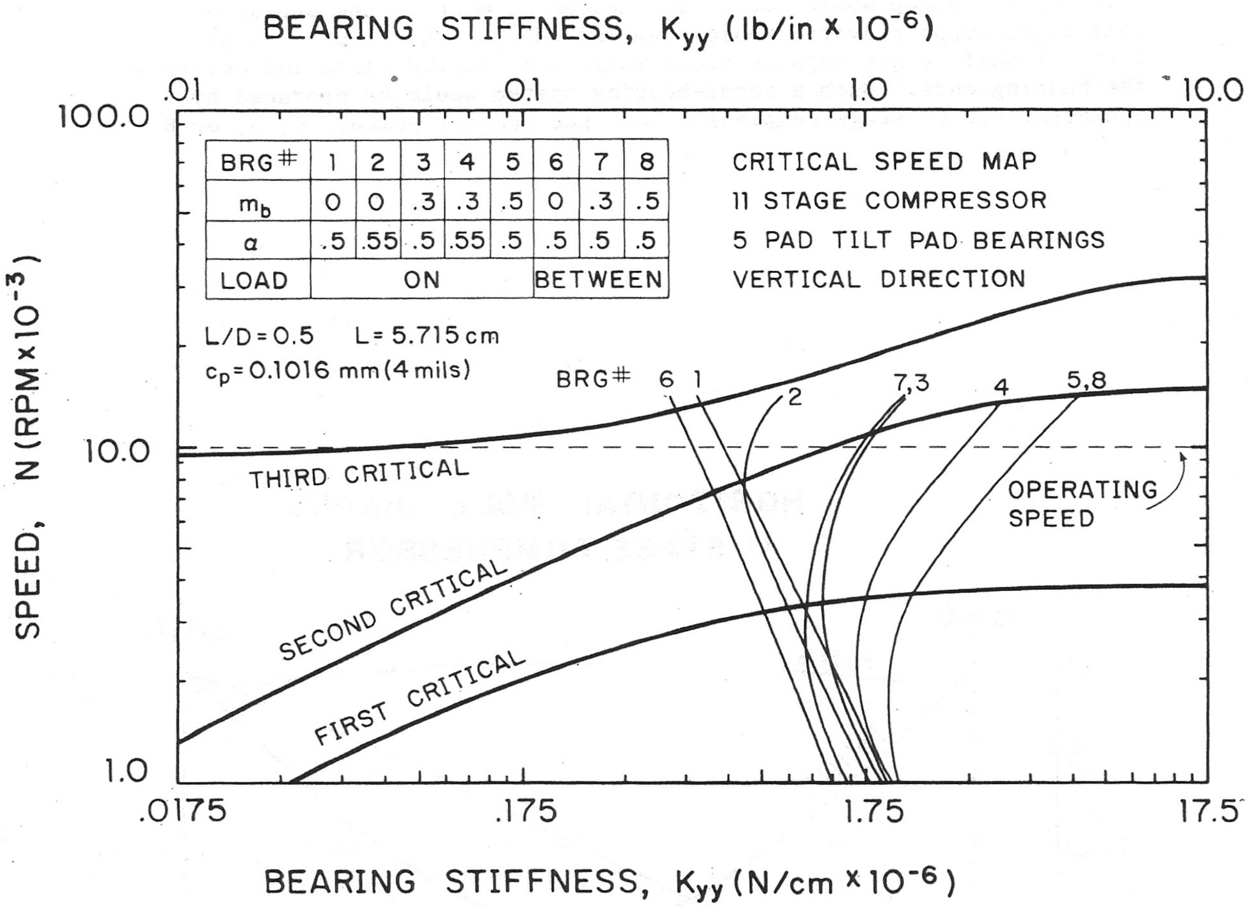

FIGURE 5 CRITICAL SPEED MAP, VERTICAL DIRECTION, 11-STAGE CENTRIFUGAL COMPRESSOR

Bearing number 1 produces the best stability characteristics for the compressor. However, its effect on unbalance response is, as yet, unknown. Figure 5 suggests that bearing number 1 may force the compressor to operate close to or on the second critical speed, especially since bearing damping will raise the undamped critical. Figures 6 and 7 show the undamped mode shapes for the 11-stage compressor operating on the number 1 five-pad bearing. The horizontal X-direction is plotted on Figure 6. Note that the first and second mode shapes are rigid-body modes. Figure 7 is a plot of the vertical Y-direction modes. Since the Y-direction stiffness is larger than the horizontal stiffness, the first and second modes are a combination of rigid-body and pure-bending mode shapes.

The effects of a tilt pad bearing on machine stability can be seen from the undamped critical speed map and undamped mode shapes. Bearing number 1 has good stability characteristics. Its bearing properties do not locate it in the "rigid support" section of the map. Its mode shapes show close resemblance to rigid-body modes. From an unbalance point of view, the mode shapes of Figures 6 and 7 suggest that they will be well damped, especially the first and second modes since a large part of the vibration occurs at the bearing locations. The bearing damping should have a large effect on the compressor system providing good unbalance characteristics as well as good machine stability. Conversely, a rotor-bearing system operating in the "rigid support" section of the critical speed map would not be influenced as much by the bearings. This rigid support system would have mode shapes that look like classical flexible shaft rigid support modes where very little vibration occurs at the bearing ends. Such a rotor-bearing system would be produced by operating the 11-stage compressor on 5-pad bearing numbers 4, 5, or 8.

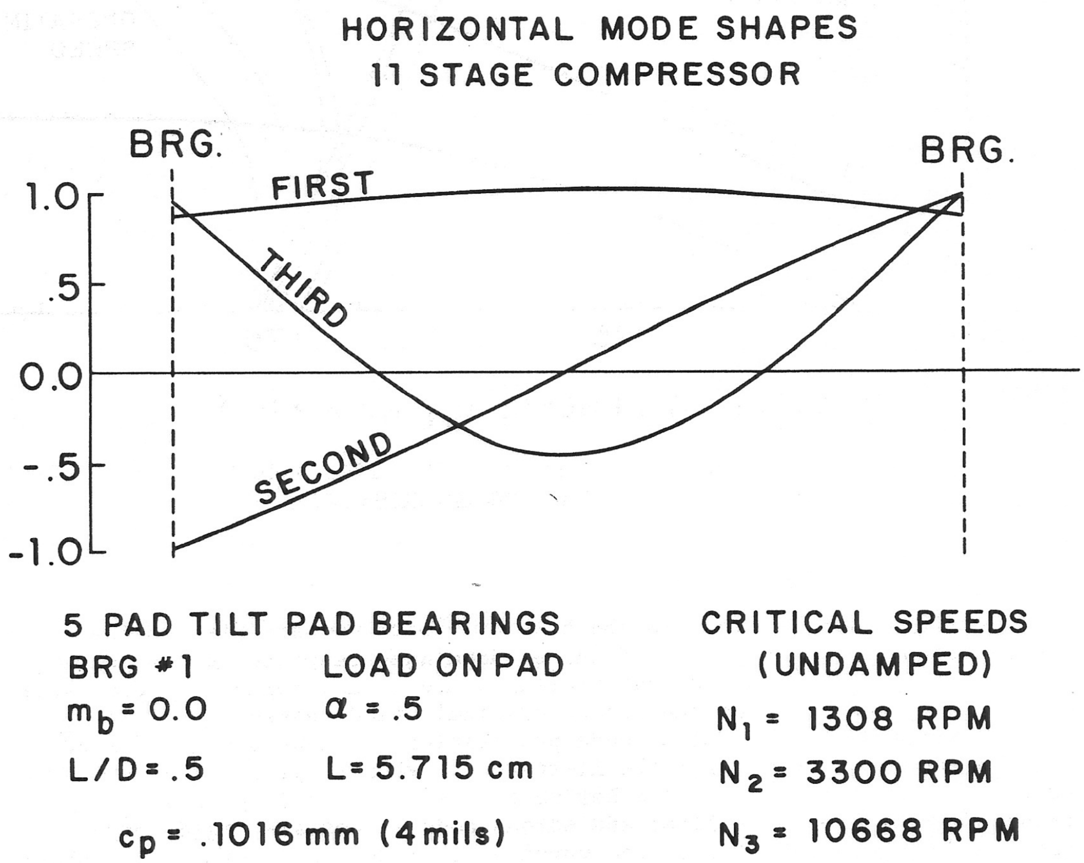

FIGURE 6 HORIZONTAL MODE SHAPES, 11-STAGE CENTRIFUGAL COMPRESSOR

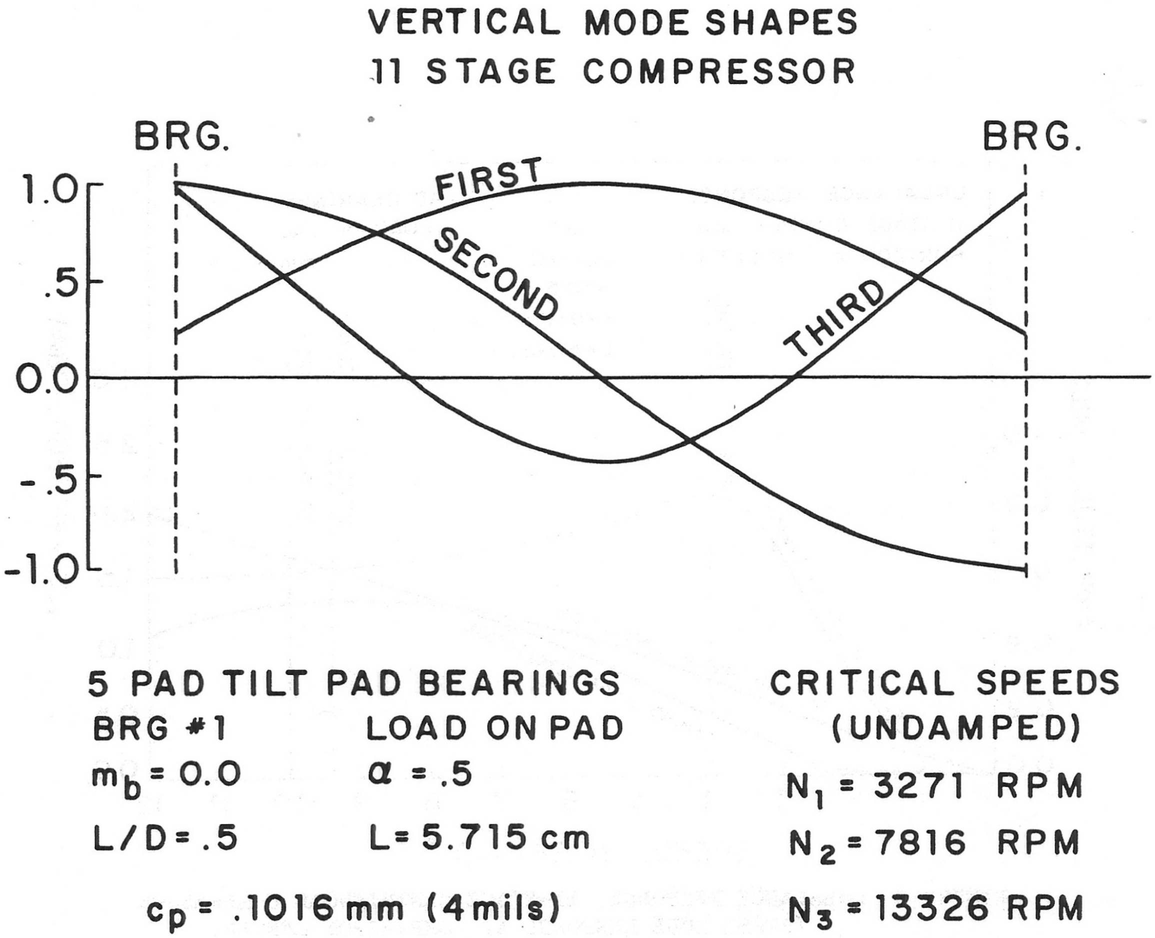

FIGURE 7 VERTICAL MODE SHAPES, 11-STAGE CENTRIFUGAL COMPRESSOR

Figure 8 shows the unbalance response of the 11-stage centrifugal compressor supported on 5-pad tilt pad bearing number 1. If it is assumed that the residual unbalance in the rotor after balancing produces an acceleration equal to one tenth of gravity, there would be 57.67 gm-cm (.73 oz-in) of unbalance remaining in the rotor. Approximately eight times as much unbalance is used to excite the compressor. Figure 8 is a plot of the first, second, and third modal excitations for the horizontal direction. The response to the first mode excitation is at the compressor center while the second and third mode excitation show the unbalance response at the bearing locations (compressor ends). The amount and location of unbalance used to produce these excitations is given in Table 6. For example, 474.0 gm-cm (6.0 oz-in) were placed in the middle of the rotor to excite the first mode. Note that damping has raised the first critical speed from 1308 RPM for the undamped case to 4000 RPM. The second critical has increased from 3300 to 9400 RPM and the third from 10668 RPM to far above the operating speed of the compressor. Even though the second critical speed is very near the operating speed of the compressor, it is certainly well damped and not easily excited even with a second mode unbalance distribution. Tilt pad bearing number 1 not only provides good stability characteristics to the compressor, but it also provides enough effective damping to give good unbalance response characteristics.

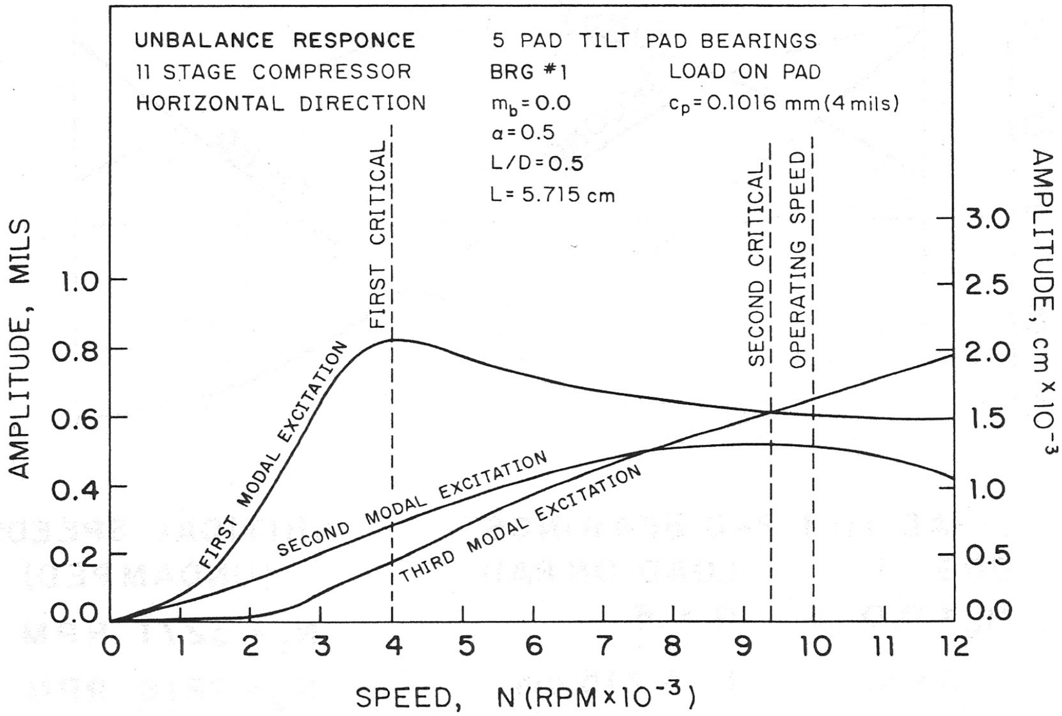

FIGURE 8 UNBALANCE RESPONSE, 11-STAGE CENTRIFUGAL COMPRESSOR (FIRST MODE RESPONSE AT COMPRESSOR CENTER, SECOND AND THIRD MODE RESPONSE AT BEARING LOCATIONS)

MODAL EXCITATION	AMOUNT AND PHASE OF UNBALANCE		
	LEFT END	CENTER	RIGHT END
FIRST	0.0	474 gm-cm @ 0°	0.0
SECOND	237 gm-cm @ 0°	0.0	237 gm-cm @ 180°
THIRD	158 gm-cm @ 0°	158 gm-cm @ 180°	158 gm-cm @ 0°

TABLE 6 AMOUNT AND LOCATION OF UNBALANCE USED TO EXCITE THE 11-STAGE COMPRESSOR

Bearing Number	m_b	c_p		c_b	
		mm	mils	mm	mils
1, 2, 6	0.0	.1016	4.0	.1016	4.0
3, 4, 7	0.3	.1016	4.0	.07112	2.8
5, 8	0.5	.1016	4.0	.0508	2.0

TABLE 7 PRELOAD, PAD CLEARANCE AND PIVOT CLEARANCE

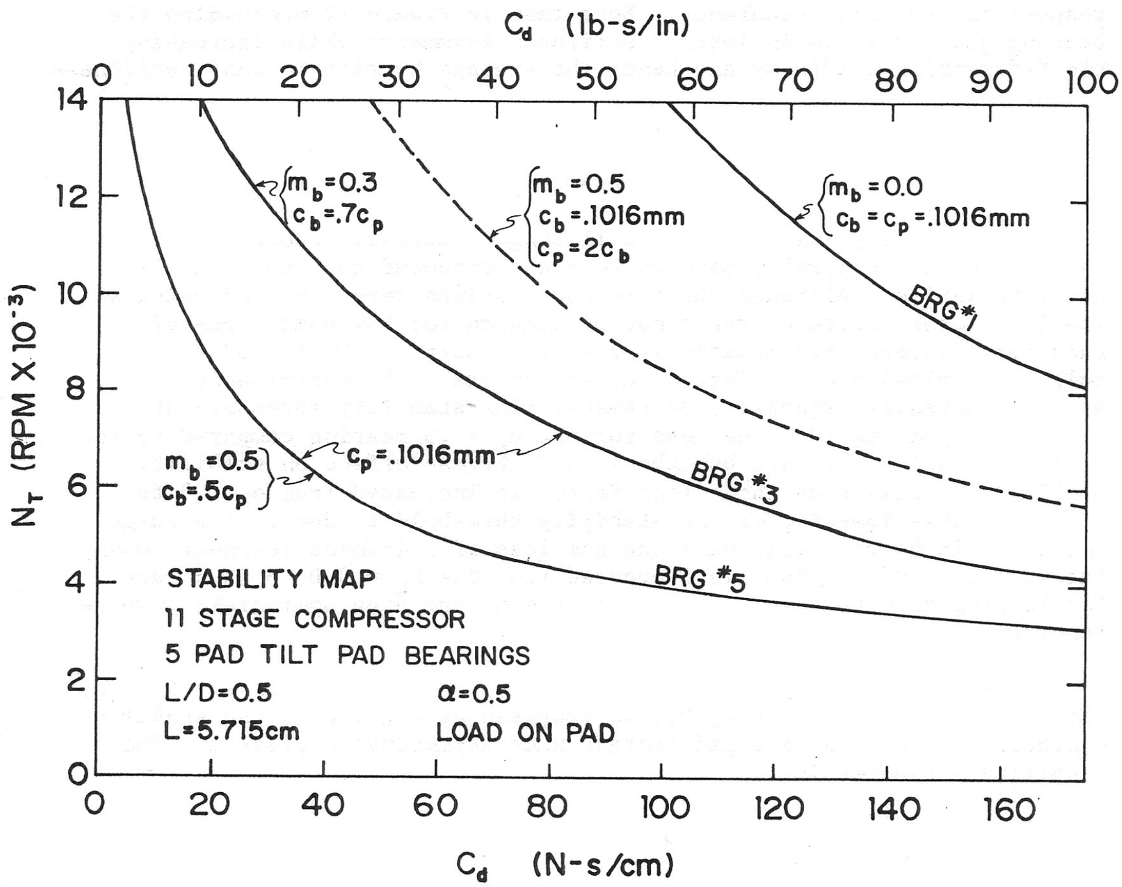

FIGURE 9 STABILITY MAP OF THE 11-STAGE COMPRESSOR COMPARING PRELOAD PERFORMANCE

PAD CLEARANCE, PIVOT CLEARANCE AND PRELOAD

The preloaded bearings discussed in the preceding sections were preloaded by varying the pivot clearance, c_b while the pad clearance, c_p is held constant (Table 7). However, preloading a bearing by varying c_p would result in different bearing characteristics compared to the preloaded bearings of Table 7 even though the preload is the same (discussions and authors' closures, references (5, 16)). This section considers a stability analysis of the 11-stage compressor supported by a pair of $m_b = 0.5$, $c_b = .1016$ mm bearings. Figure 9 illustrates the results of this analysis. The $m_b = 0.5$, $c_b = .1016$ mm bearing is shown as the dashed line. For comparison, the stability curves for bearing numbers 1, 3 and 5 are replotted in Figure 9. Preloading the bearing by increasing the pad clearance rather than decreasing the pivot clearance does improve the stability characteristics of the compressor system. This is evident by comparing the dashed line to the bearing number 5 curve in Figure 9. However, the zero preload design out performs all preloaded cases.

The relative merits of preloading a tilt pad bearing by changing the pad or pivot clearance is not a major consideration of this paper. Bearings designed to match the shaft stiffness remains the central issue. Figure 10 of the Appendix is a plot of the bearing characteristics for the zero and .5 preloaded cases normalized with respect to the pad clearance, while Figure 12 considers the same two cases normalized with respect to the pivot clearance. Note that in Figure 12 preloading the bearing still results in loss of stiffness asymmetry while increasing the X-direction stiffness and hence the average bearing to shaft stiffness ratio.

CONCLUSIONS

The stability analysis of the 11-stage compressor shows that the zero preloaded, centrally-pivoted bearings produced the best stability characteristics. Although the tilt pad bearings were compared using a specific rotor, certain trends may be deduced for the same class of machinery (rotors with relatively flexible shafts). These deductions follow. Preload has the largest effect on stability performance. As preload increases, stability decreases. The stability threshold at operating speed is 10 times less for the $m_b = .5$ bearing compared to the $m_b = 0.0$ bearing. Offset has the second largest effect on stability. Stability decreases as the offset factor is increased from $\alpha = .5$ to $\alpha = .55$. This lowering of the stability threshold is due to the large increases in bearing stiffness and the loss of stiffness asymmetry when the preload and/or offset is increased from the $m_b = 0.0$, $\alpha = .5$ case. Pad loading effects stability very little at the high Sommerfeld numbers considered here.

A stability parameter based on the shaft flexibility ratio, R_s, and the bearing asymmetry ratio, R_f, is proposed as a guide to the stability characteristics of a tilt pad bearing when asymmetry is present. The stability parameter is

$$P_s = 2R_s |1 - R_f|$$

Approximate stability guidelines are

$P_s \geq .8$	rotor-bearing stability	good
$P_s \leq .1$	rotor-bearing stability	poor
$.1 \leq P_s \leq .8$	rotor-bearing stability	marginal

The stiffness ratio, $\bar{K}$, may also be used as a stability guide. Large $\bar{K}$ values (above 6.0) imply that the rotor-bearing system will exhibit poor stability characteristics. Stiffness ratio values of around 1.0 or 2.0 result in favorable stability characteristics.

A measure of the amount of damping supplied to the rotor system by the bearing damping and shaft stiffness is the effective damping ratio. As effective damping increases, stability characteristics increase. Also, increasing effective damping means improving the unbalance response characteristics of the rotor-bearing system. Improving system stability also improves the unbalance response characteristics.

Insight into the stability and unbalance response of a rotor-bearing system may be deduced from the undamped critical speed mode shapes and the critical speed maps. If the bearing stiffness curve is near the rigid support section of a critical speed map, then the bearing would provide unfavorable stability and unbalance characteristics to the rotor-bearing system. Conversely, if the bearing stiffness curve is near the rigid rotor section of the map, then this bearing would provide favorable stability and unbalance characteristics. Similarly, if the rotor-bearing systems mode shapes are nearly rigid-body modes, then the bearings would provide favorable stability and unbalance characteristics. Modes that are nearly classical bending mode shapes would infer that the bearings provide poor stability and unbalance characteristics.

The proper choice of a tilt pad bearing is very important if good stability and unbalance response characteristics are to be expected. A poor choice does not provide enough effective damping to operate the rotor at the running speed without the rotor going unstable. The key to this entire analysis is to tune the bearing to match the shaft stiffness. For multimass rotors with very flexible shafts, the bearings must be designed to be as flexible as possible to insure good operating characteristics. Since there are so many design variables available for tilt pad bearings (clearance, preload, offset, pad loading, number of pads, etc.) proper bearing design is, in many cases, attainable. For the example considered here, the zero preloaded, centrally-pivoted bearing provided the best characteristics. Many people are reluctant to use the zero preload design since the top pads may "lock up." This may be eliminated by beveling the leading edge of the pads to allow converging oil flow regardless of pad pitch. However, proper design might possibly be obtained by varying the pad clearance and/or the number of pads.

APPENDIX

Figures 10, 11 and 12 show stiffness and damping coefficients for bearing numbers 1, 5, 7, and 8. Figure 12 is a replot of Figure 10 with the data normalized with respect to the pivot clearance, c_b instead of the pad clearance c_p. These curves are part of the data illustrated in reference (16) and (20). The finite element matrix approach (19) is used to solve for the hydrodynamic pressures for the single fixed pad. A Newton-Raphson iterative scheme is employed to determine the equilibrium position of the single pad. This iterative scheme due to its fast convergence permits the determination of an accurate equilibrium position. Small numerical perturbations about this position in displacement and velocity determines the characteristics of the single pad. The pad assembly method is used to calculate the stiffness and damping coefficients of the full tilt pad bearing (4, 16). The effects of the top, unloaded pads are included.

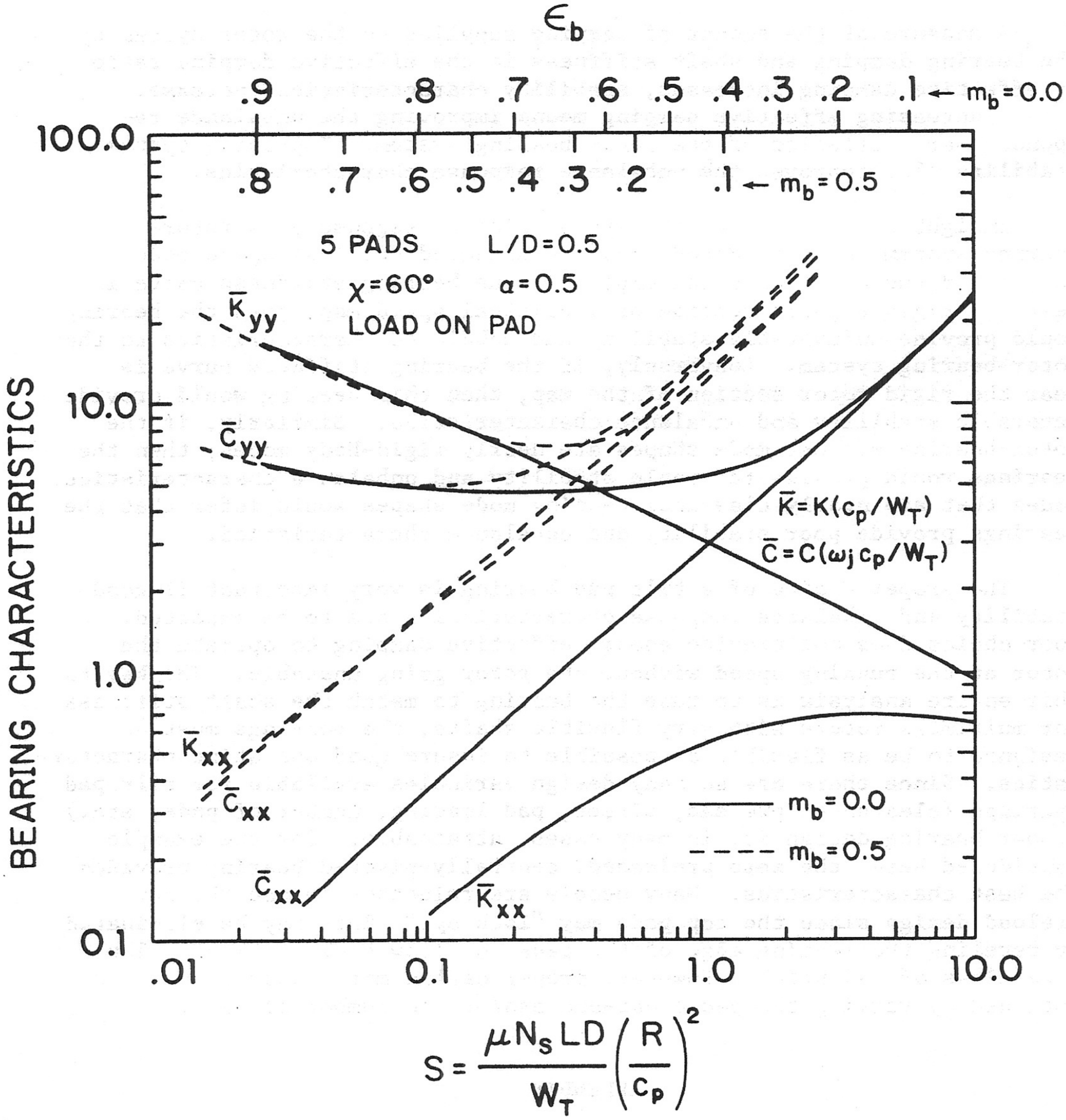

FIGURE 10 TILT PAD BEARING CHARACTERISTICS
(BEARING NUMBER 1, m_b = 0.0 AND BEARING NUMBER 5, m_b = 0.5)

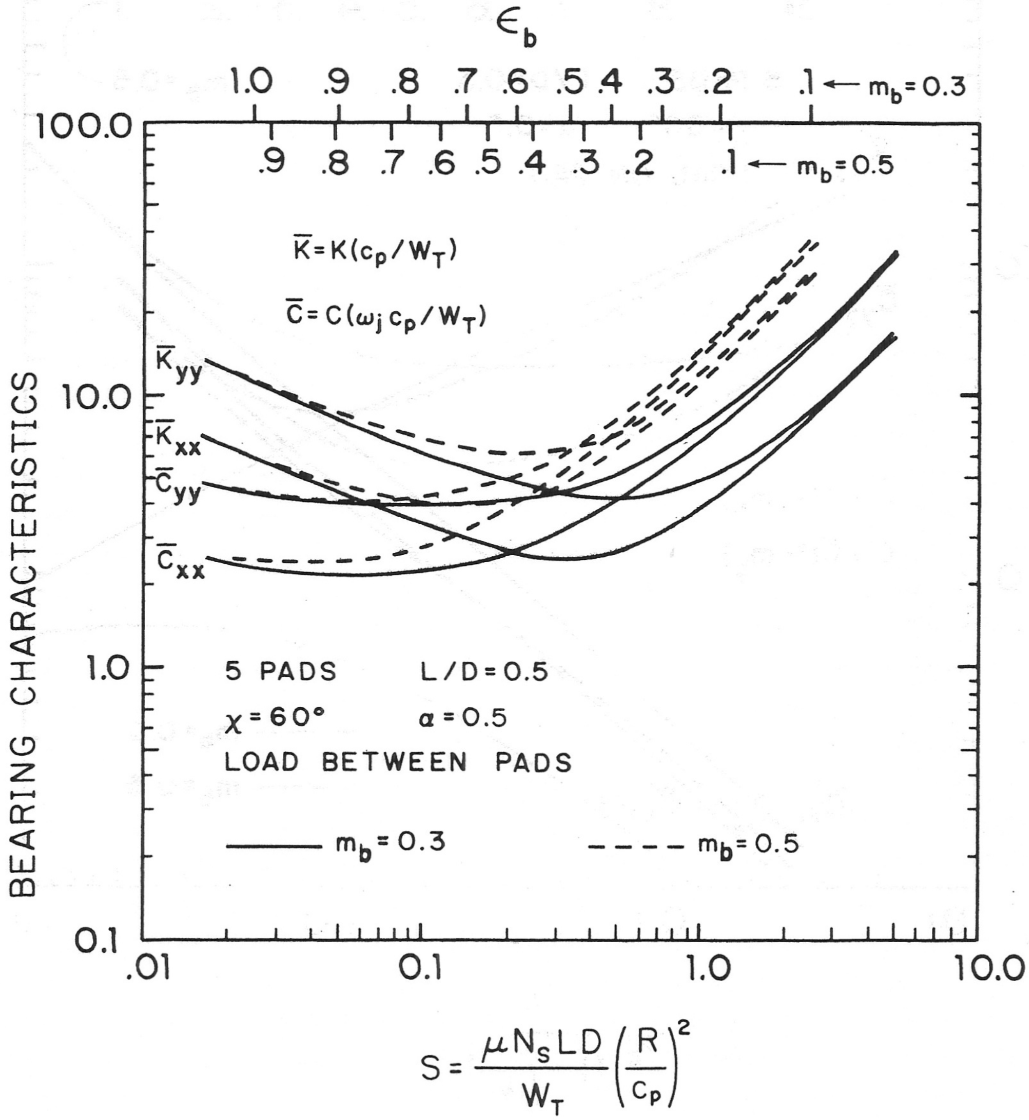

FIGURE 11 TILT PAD BEARING CHARACTERISTICS
(BEARING NUMBER 7, m_b = 0.3 AND BEARING NUMBER 8, m_b = 0.5)

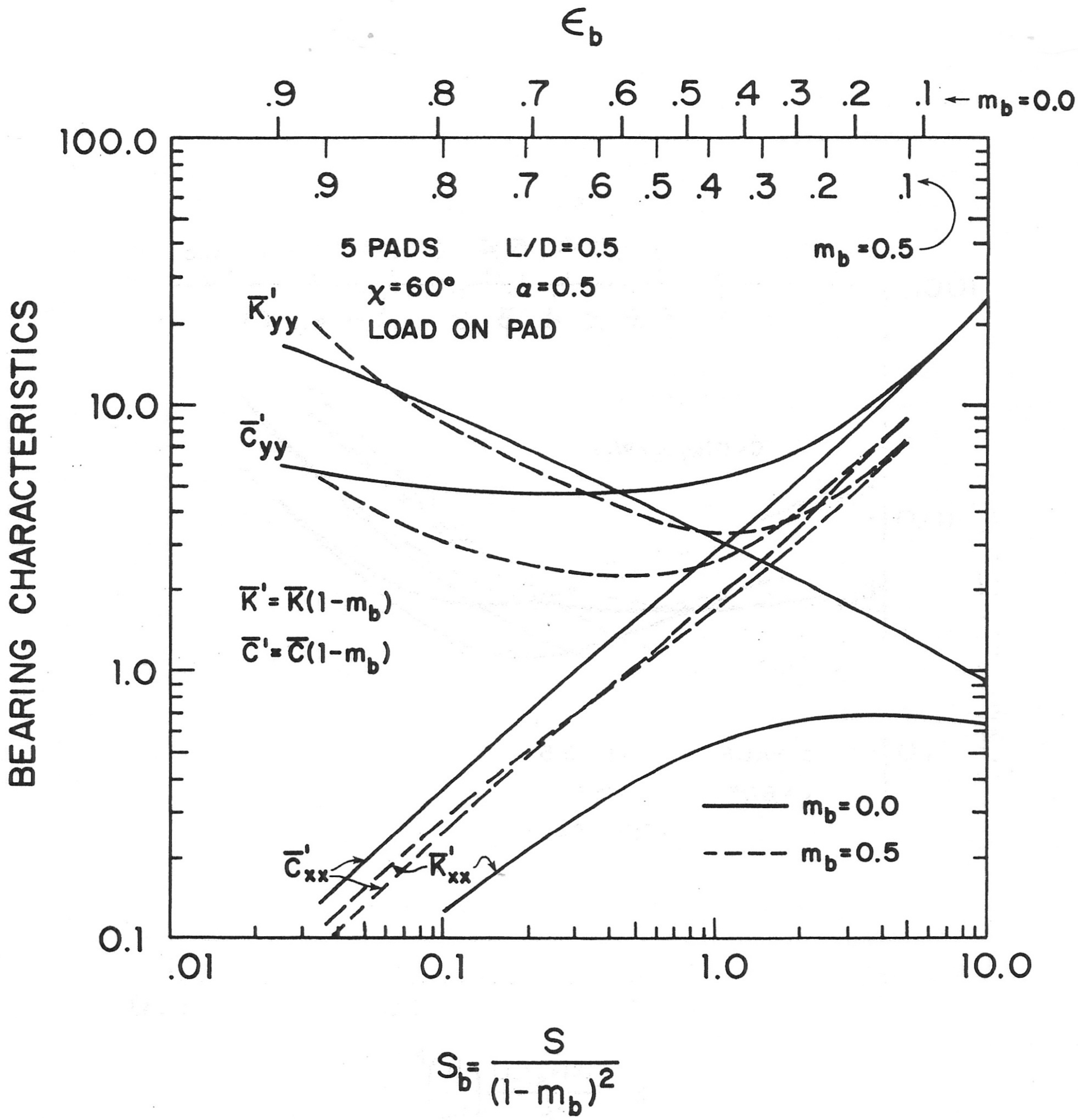

FIGURE 12 TILT PAD BEARING CHARACTERISTICS FROM FIGURE 10 NORMALIZED WITH RESPECT TO THE PIVOT CLEARANCE, c_b

REFERENCES

1 Poritsky, H., "Contribution to the Theory of Oil Whip," Trans. ASME, August, 1953, pp. 1153-1161.

2 Hori, Y., "A Theory of Oil Whip," Journal of Applied Mechanics, ASME, June, 1959, pp. 189-198.

3 Lund, J. W., Saibel, E. "Oil Whip Whirl Orbits of a Rotor in Sleeve Bearings," Journal of Engineering for Industry, Trans. ASME, Vol. 89, No. 4, pp. 813-823, November, 1967.

4 Lund, J. W., "Spring and Damping Coefficients for the Tilting-Pad Journal Bearing," American Society of Lubrication Engineers Transactions, Vol. 7, No. 4, October, 1964, pp. 342-352.

5 Orcutt, F. K., "The Steady State and Dynamic Characteristics of the Tilting Pad Journal Bearing in Laminar and Turbulent Flow Regimes," Journal of Lubrication Technology, Trans. ASME, Series F, Vol. 89, No. 3, July, 1967, pp. 392-404.

6 Alford, J. S., "Protecting Turbomachinery from Self-Excited Rotor Whirl," Journal of Engineering for Power, Trans. ASME, No. 4, October, 1965, pp. 333-344.

7 Warner, R. E., Soler, A. I., "Stability of Rotor-Bearing Systems with Generalized Support Flexibility and Damping and Aerodynamic Cross-Coupling," Journal of Lubrication Technology, Trans. ASME, Vol. 97, No. 3, July, 1975, pp. 461-471.

8 Lund, J. W., "Stability and Damped Critical Speeds of a Flexible Rotor in Fluid-Film Bearings," Journal of Engineering for Industry, Trans. ASME, Vol. 96, No. 2, May, 1974, pp. 509-517.

9 Gunter, E. J., "Rotor-Bearing Stability," Proceedings of the First Turbomachinery Symposium, Texas A & M University, College Station, Texas, October, 1972, pp. 119-141.

10 Robertson, D., "Hysteretic Influences on the Whirling of Rotors," Proceedings of the Institute of Mechanical Engineers, London, Vol. 131, 1935, p. 513.

11 Gunter, E. J., "The Influence of Internal Friction on the Stability of High-Speed Rotors," Journal of Engineering for Industry, Trans. ASME, Vol. 89, November, 1967, pp. 683-688.

12 Gunter, E. J., Trumpler, P. R., "The Influence of Internal Friction on the Stability of High-Speed Rotors with Anisotropic Supports," Journal of Engineering for Industry, Trans. ASME, Vol. 91, No. 4, November, 1969, pp. 1105-1113.

13 Black, H. F., "The Stabilizing Capacity of Bearings for Flexible Rotors with Hysteresis," Journal of Engineering for Industry, Trans. ASME, February, 1976, pp. 87-91.

14 Ehrich, F. F., "Shaft Whirl Induced by Rotor Internal Damping," Journal of Applied Mechanics, Trans. ASME, June, 1964, pp. 279-283.

15 Gunter, E. J., Barrett, L. E., and Allaire, P. E., "Design of Nonlinear Squeeze-Film Dampers for Aircraft Engines," Journal of Lubrication Technology, Trans. ASME, Vol. 99, No. 1, January, 1977, pp. 57-64.

16 Nicholas, J. C., Gunter, E. J., Allaire, P. E., "Stiffness and Damping Coefficients for the Five-Pad Tilting Pad Bearing," accepted by ASLE for publication, preprint no. 77-LC-3A-2, October, 1977.

17 Elwell, R. C., and Findlay, J. A., "Design of Pivoted-Pad Journal Bearings," Journal of Lubrication Technology, Trans. ASME, Vol. 91, No. 1, January, 1969, pp. 37-103.

18 Barrett, L. E., Gunter, E. J., Allaire, P. E., "Optimum Bearing and Support Damping for Unbalance Response and Stability of Rotating Machinery," Journal of Engineering for Power, Trans. ASME, ASME paper No. 77-GT-27.